

Phase behaviour and sol–gel transition of poly(vinyl alcohol)–borate complex in aqueous solution

Hidenobu Kurokawa, Mitsuhiro Shibayama*, Takeshi Ishimaru and Shunji Nomura

Department of Polymer Science and Engineering, Kyoto Institute of Technology, Matsugasaki, Sakyo, Kyoto 606, Japan

and Wel-li Wu

National Institute of Standards and Technology, Gaithersburg, MD 20899, USA
(Received 12 March 1991; revised 9 May 1991; accepted 20 May 1991)

Phase behaviour and sol–gel transition of poly(vinyl alcohol) (PVA) aqueous solutions in the presence of borate ions were investigated. PVA molecules are known to form charged complexes with borate ions in aqueous solutions containing borax ($\text{Na}_2\text{B}_4\text{O}_7 \cdot 10\text{H}_2\text{O}$) or a mixture of boric acid and sodium hydroxide. These complexes show the following viscosity and phase behaviour as a function of the concentrations of boric acid, sodium hydroxide, and salt.

1. At a given combination of PVA concentration and ionic strength, the system underwent a clear–opaque–clear transition with increasing boric acid concentration.
2. The intrinsic viscosity $[\eta]$ decreased first and then increased with increasing boric acid concentration in alkaline solution.
3. The opaque region grew to some extent with time and/or by adding salt (i.e., NaCl).
4. When the polymer concentration increased, a thermoreversible sol–gel transition took place without phase demixing. The gelation concentration was close to the chain overlap concentration estimated from $[\eta]$.

All the above phenomena can be explained by a balance of the excluded volume effect due to intra- and inter-chain crosslinks and electrostatic potentials.

(Keywords: phase behaviour; poly(vinyl alcohol); complexes)

INTRODUCTION

The gelation of poly(vinyl alcohol) (PVA) has been studied extensively in recent years^{1–11}. Several gelation mechanisms have been reported, such as chemical reactions with various ions (borate¹², titanate¹³, cupric¹⁴, antimonate¹⁵, etc.) and crystallization in spite of the atactic nature of PVA. The mechanism of ion-assisted crosslinks of PVA is believed to be a so-called ‘di-diol’ complexation, which is formed between two diol units and one borate ion¹².

Recently, we proposed an alternative model for this complex based on ¹¹B-n.m.r. experiments⁶. Sinton⁴ and Pezron *et al.*^{16,17}, however, supported the ‘di-diol’ complex model from their ¹¹B-n.m.r. work. In both models, it appears that two diol units of PVA chains react with one borate ion to form a crosslink. This phenomenon depends on the concentrations of the reactants, such as PVA concentration, C , borate ion concentration, b , and temperature, T . In our previous paper⁷, the gel melting temperature of PVA/boric acid/NaOH aqueous solutions was evaluated as a function of C , b , the degree of polymerization of PVA, P , and pH. It was found that two moles of diol units of PVA react with one mole of borate ions, and the gel melting temperature, T_{gel} , satisfied the following

equation:

$$\ln[CPb] = (\text{constant}) + \Delta H/RT_{\text{gel}} + \ln\{([\text{H}^+] + K_a)/K_a\} \quad (1)$$

where ΔH , $[\text{H}^+]$, K_a , and R are the enthalpy of crosslink formation, the proton concentration, the ionization constant of boric acid, and the gas constant, respectively. It should be noted here that T_{gel} is identical to the sol–gel transition temperature in this particular case because the system undergoes a thermoreversible sol–gel transition without significant thermal hysteresis.

The PVA–borate crosslinking mechanism is divided into two reactions, as shown in *Figure 1*; a monodiol complexation (reaction I) and a crosslink formation (reaction II). Once a borate ion is attached to a polymer chain (reaction I), the polymer chain behaves as a polyelectrolyte unless the borate ion is removed from the chain or is bound to another diol unit as a crosslinking point. In this case, a significant contribution of electrostatic repulsion between monodiol units is expected, resulting in an expansion of the individual polymer chains. In reaction II, the dimension of the chain is lowered due to crosslink formation, and a collapse transition may also be expected if the polymer–polymer attractive interaction is greater than the polymer–solvent interaction. In other words, the chain dimension and the stability of the system is ruled by these two antagonistic

*To whom correspondence should be addressed

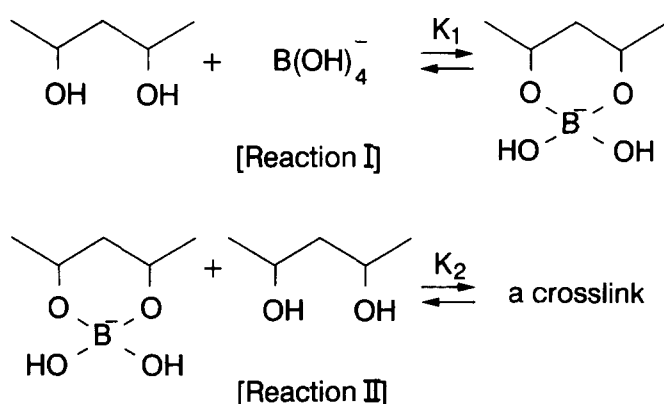


Figure 1 PVA–borate crosslinking mechanism: reaction I, monodiol complexation; and reaction II, crosslink formation

reactions. Hence, the PVA–borate ion systems provide several interesting problems: solubility; complexation equilibria; polyelectrolyte effects; reversible crosslinking, and so on. Leibler *et al.*¹⁸ discussed these problems based on Ochiai's data¹⁹ on a PVA–borax system, and proposed a theory to predict the equilibrium size of the individual polymer chain. They showed that the dimension of the individual polymer chain was given by a balance of the elastic energy, the excluded volume effect, and the electrostatic potential. Pezron *et al.*²⁰ studied the phase behaviour and obtained C^* (chain overlap concentration) for a galactomannan–borax system, which is also a polyhydroxy polymer capable of complexation.

In this paper, we will consider: the relationship between the gelation concentration and C^* ; the clear–opaque–clear transition; and the effect of added salt on phase behaviour, in terms of viscometry and phase diagrams. The spatial inhomogeneity in PVA/boric acid/NaOH systems was investigated by small angle neutron scattering, and the results will be reported shortly^{21,22}.

EXPERIMENTAL

Samples

Re-saponified poly(vinyl alcohol)s (PVAs) with degrees of polymerization, P , of 1100 and 1800 were used. For both samples, the degrees of saponification were more than 99.9 mol%. The details of the microstructure of PVAs have been described elsewhere⁷.

Viscosity measurements

Viscosity measurements were carried out using a Ubbelohde capillary viscometer at $60 \pm 0.05^\circ\text{C}$. This temperature was relatively high compared with the conventional viscosity measurement for PVA, i.e., 30°C . The temperature was chosen to avoid phase demixing during measurement, and to lower the viscosity of the sample solutions particularly for semi-dilute solutions ($> 5 \text{ g l}^{-1}$).

Phase diagram

The desired amounts of PVA, boric acid, NaOH aqueous solutions were mixed in a test tube and heated in a water bath at 95°C until a homogeneous solution was obtained. Most of the samples, except those containing a high concentration of added salt, gave

homogeneous, clear solutions. The samples were then kept in a temperature controlled chamber at 17°C . The sol–gel transition was determined by inverting the test tube after 30 min of sample preparation. The samples were retained in the chamber until phase behaviour had been examined. The demixing transition was detected for some samples by visual observation after a given time. Demixed samples differed from the others in being opaque during the time period of observation.

RESULTS AND DISCUSSION

Phase diagram

Figure 2 shows the phase diagram of PVA ($P = 1100$) aqueous solutions containing NaOH and $\text{B}(\text{OH})_3$ at 17°C . The parameters C and b denote the concentrations of PVA and boric acid, respectively. The NaOH concentration was 0.167 mol l^{-1} , which was sufficiently high to maintain the system pH at around 13. Most of the boric acid molecules ionize since the $\text{p}K_a$ is ~ 9.0 . The times of observation after sample preparation are given in the figure, i.e., 48 and 150 h. A clear–opaque–clear transition was observed when the boric acid concentration was increased at $C \geq 5 \text{ g l}^{-1}$. The opaque region grew with time to some extent. Although observation was continued for 330 h, no further change in the demixing line was detected.

The sol–gel phase boundary was determined before demixing occurred. After demixing, the sol–gel boundary shifted to the lower polymer concentration side in the demixing zone. However, it was difficult to distinguish sol from gel since a syneresis was observed, and two phases were present in the system, i.e., an opaque polymer-rich gel region and a clear dilute polymer solution. The sol–gel phase boundary that was determined before demixing may be explained by taking account of C^* at which the polymer chains start to overlap each other. The boundary after demixing could be explained by the gelation behaviour induced by

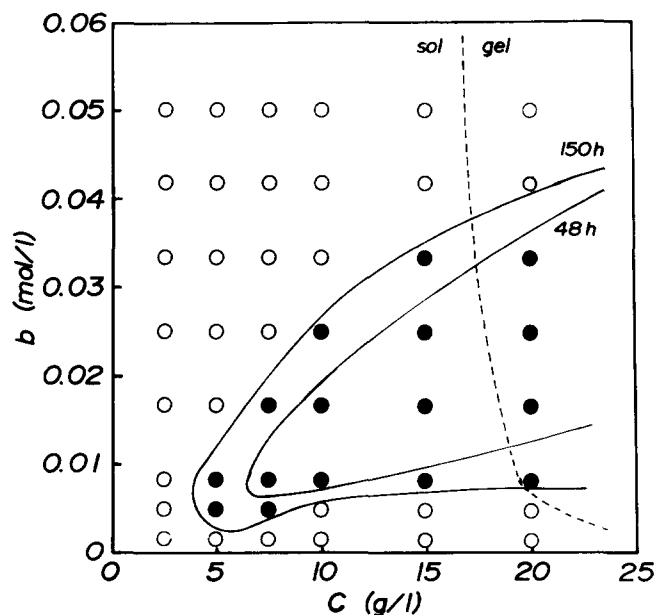


Figure 2 Phase diagram of PVA ($P = 1100$) aqueous solutions at 17°C . NaOH concentration = 0.167 mol l^{-1} . ○, Clear system; ●, opaque system; —, phase mixing lines at given times; ---, sol–gel transition line observed after 30 min of sample preparation

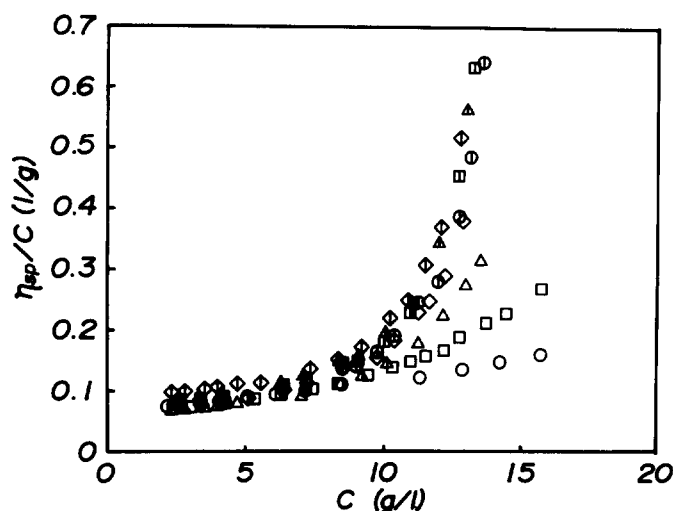


Figure 3 Plots of η_{sp}/C versus C for PVA ($P = 1800$) aqueous solutions containing different concentrations of boric acid, b : ○, 0.00208; □, 0.00417; △, 0.00833; ◇, 0.0167; ⊕, 0.0250; ⊞, 0.0333; ⊕, 0.0417; ⊕, 0.0500 mol l⁻¹

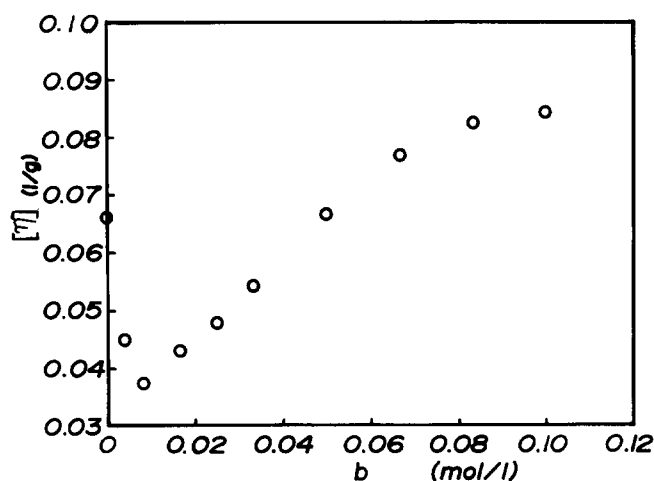


Figure 4 Boric acid concentration b , dependence on intrinsic viscosity, $[\eta]$. $P = 1800$; NaOH concentration = 0.167 mol l⁻¹

liquid–liquid phase separation^{3,23}. In this paper, we will not discuss the sol–gel phase boundary after demixing since it could not be determined precisely, but we will focus on the phase boundary before demixing and the demixing behaviour of this system.

Viscosity behaviours

Figure 3 shows the plot of η_{sp}/C versus C for PVA solutions having different boric acid concentrations, b , where η_{sp} is the specific viscosity. The concentration of NaOH was fixed at 0.167 mol l⁻¹ and the degree of polymerization of PVA was 1800. At low PVA concentrations, there is no significant difference in η_{sp}/C . However, at $C > 10$ g l⁻¹, the viscosity behaviour depends on b . For solutions having low b values, the increase in η_{sp}/C with C is relatively slow, whereas those having $b > 0.0083$ mol l⁻¹ show some divergence. Viscosity measurements at higher PVA concentrations were not studied due to the limitations of the capillary-type viscometer.

The intrinsic viscosity, $[\eta]$, was estimated by extrapolating the η_{sp}/C versus C curves to $C = 0$. Figure 4 shows the dependence of b on $[\eta]$. It is interesting that $[\eta]$ decreases at low b and then increases with b . A similar phenomenon was reported by Ochiai *et al.*¹⁹, and was explained by Leibler *et al.*¹⁸ in terms of the free energy change of a polymer chain capable of intra-chain crosslinking in the presence of an electrostatic potential. At low values of b , each PVA chain tends to contract or collapse, due to the formation of intra-molecular crosslinking. Since the number of monodiol complexes on a chain increases with an increase in b , Coulombic repulsion between borate ions tagged on a PVA chain expands the chain. This behaviour is related to the clear–opaque–clear transition shown in Figure 2.

C_{gel} was estimated by assuming a power law divergence, i.e.

$$\eta = A[(C_{gel} - C)/C_{gel}]^{-t} \quad (2)$$

where A and t are constants. We expect that values of C_{gel} are given as concentrations where chains start to overlap each other (C^*). Since the chain overlap concentration, C^* , is given by

$$C^* \approx 1/[\eta] \quad (3)$$

both C_{gel} and C^* can be estimated from viscosity measurements using equations (2) and (3). Figure 5 shows the dependence of b on C_{gel} and C^* . At low boric acid concentrations ($b < 0.00833$ mol l⁻¹), C_{gel} diverges because the concentration of crosslinkers is not high enough. At $b > 0.00833$ mol l⁻¹, the values of C_{gel} tend to remain constant rather than to follow the values of C^* . The constant value can be regarded as identical to that of C^* at $b = 0$. As can be seen in equation (3), C^* is estimated from $[\eta]$, i.e., the chain dimension at the infinite dilution of the polymer concentration. In the case of neutral polymers, the lowest polymer concentration at which the system undergoes gelation, i.e., C_{gel} , might be identical to C^* . On the contrary, in the case of ionized polymer chains, intra- and inter-chain interactions including crosslink formations disturb the chain dimension, resulting in some deviation of C_{gel} from C^* . Hence C_{gel} may deviate from C^* to some extent. The results shown in Figure 5 indicate that the dimension of a chain that is in a semi-dilute region is not very sensitive

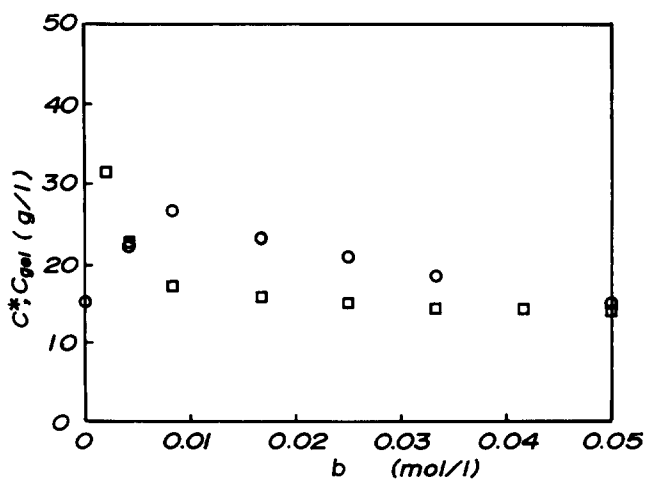


Figure 5 Boric acid concentration, b , dependence on gelation concentration, C_{gel} , and chain overlap concentration, C^* . $P = 1800$; NaOH concentration = 0.167 mol l⁻¹; ○, C^* ; □, C_{gel}

to changes in boric acid concentration, although the number of individual chains in the dilute polymer region changes drastically with boric acid concentration.

The exponent t was estimated to be ~ 0.7 . This value seems to be in good agreement with that predicted by the percolation model²⁴. The main purpose of this work, however, is not to discuss the critical phenomenon of this system. More precise experiments to estimate the exponent and C_{gel} are now in progress.

Demixing transition

The demixing transition of polymer aqueous solutions was studied by Pezron *et al.*²⁰. They worked on galactomannan aqueous solutions containing borax. They observed a clear–opaque transition. We will now discuss the clear–opaque–clear transition more quantitatively based on the theory of a polymer chain dimension capable of complexation, which has been proposed by Leibler *et al.*¹⁸.

This system can be treated as a random copolymer composed of borate-free diol units and borate-bonded diol units. The fraction of the borate-free and borate-bonded diol units are f_0 and f_1 , respectively,

$$f_0 = C_P/C, \quad f_1 = C_{PM}/C \quad (4)$$

where

$$C_{PM} = K_1 C_P C_M \quad (5)$$

$$C_{PMP} = K_1 K_2 C_P^2 C_M \quad (6)$$

$$C = C_P + C_{PM} + 2C_{PMP} \quad (7)$$

$$b = C_M + C_{PM} + C_{PMP} \quad (8)$$

C_P , C_{PM} , and C_{PMP} are, respectively, the concentrations of the borate-free diol units, monocomplexes, and crosslinks. C denotes the concentration of the diol units of PVA. b and C_M are the total borate ion concentration and the free borate ion concentration, respectively. K_1 and K_2 are the monocomplexation and dicomplexation constants, respectively. Note that both K_1 and K_2 are assumed to be independent of the conditions of the system, for example, the polymer concentration, ionic strength and so on. As stated previously^{18,25}, the apparent complexation constant decreases with increasing borate ion, especially in a low ionic strength region ($< 10^{-2}$ mol l⁻¹). In this work, however, the system contains relatively high concentrations of ions ($> 10^{-1}$ mol l⁻¹). Therefore, the complexation constants can be regarded as constant values.

The free energy of the system per chain is given by

$$F/kT \simeq (1/2)v_{eff}(N^2/r^3) + (1/6)w^2(N^3/r^6) \quad (9)$$

where

$$v_{eff} = vf_0^2 + vf_0f_1 + v'f_1^2 - 2(\Delta H/kT)K_2f_0f_1 \quad (9')$$

r , N , and k are the dimension of a polymer chain, the number of segments of a chain and the Boltzmann constant, respectively. v and w^2 are monomer virial coefficients of second and third orders. v' and ΔH denote the excluded volume with additional Coulombic interaction, and the enthalpy of crosslink formation, respectively. The first, second and third terms of the right-hand side (RHS) of equation (9') contribute to an expansion of the chain, if $v > 0$. The excluded volume parameter between the diol unit and the monocomplex unit was assumed to be the same as that between two

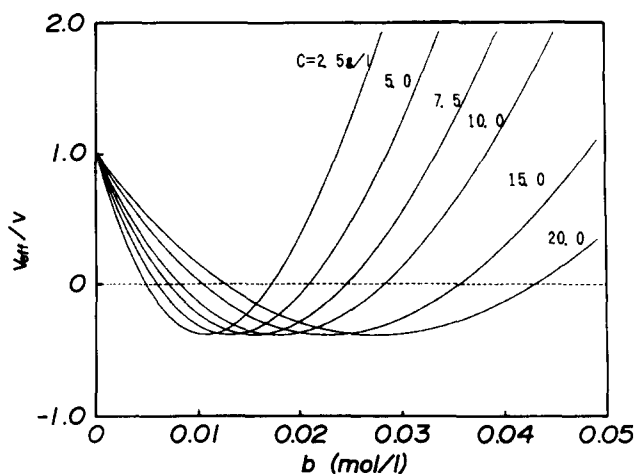


Figure 6 Boric acid concentration dependence on (v_{eff}/v) for different values of C

diol units. The value of v' is obtained by¹⁸

$$v' \simeq 4\pi Q\kappa^{-2} \quad (10)$$

$$\kappa^2 = 8\pi N_A QI \quad (11)$$

where κ^{-1} , Q , and N_A are the Debye screening length, the Bjerrum length, and Avogadro's number, respectively. I is the ionic strength consisting of the salt concentration, C_S , and the free borate ion concentration, C_M , as follows,

$$I = C_S + C_M \quad (12)$$

In this particular system, NaOH, which was added in order to adjust pH, should be considered as the salt. Q was chosen to be 7 Å as a typical value for the Bjerrum length in water at 25°C.

The phase stability can be predicted by taking the second derivative of F with respect to r , i.e., $(d^2F/dr^2) = 0$. Hence

$$(v_{eff}/v) + (7/6)(\omega^2/v)(N/r^3) = 0 \quad (13)$$

In a good solvent, the term $(\omega^2/v)(N/r^3)$ is of the order of the monomer volume fraction, and gives negligible contribution to equation (13).

Figure 6 shows the boric acid concentration dependence of (v_{eff}/v) for several cases having different polymer concentrations. K_1 was chosen¹⁸ to be 11 l mol⁻¹. Since K_2 was unknown, it was chosen as a fitting parameter, and determined to be 0.02 l mol⁻¹. v was estimated from the following equation,

$$v = a^3(1 - 2\chi) \quad (14)$$

where χ is the Flory interaction parameter. The value of χ at room temperature was determined by a set of small angle neutron scattering (SANS) measurements of PVA aqueous solutions without borate ions. The value was found to be 0.477 (ref. 26). The segment length, a , should be based on the diol unit instead of the monomer unit of PVA. Hence, we employed $a = 2^{1/2}a_{monomer}$ and $a_{monomer}$ was chosen to be the value (5.96 Å) evaluated by a SANS experiment²⁷. The enthalpy of crosslink formation, ΔH , has been reported previously^{4,7}. A value of $\Delta H = 8$ kcal mol⁻¹ was used in this work.

At $b = 0$, $f_0 = 1$, and $f_1 = 0$, hence the RHS of equation (9') becomes unity. By increasing b , the fourth term of the RHS of equation (9') becomes dominant, resulting in $v_{eff}/v < 0$. By further increases in b , a positive

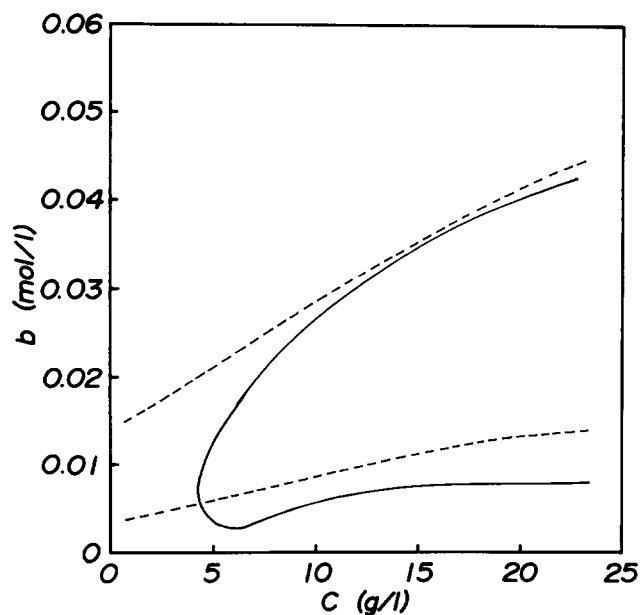


Figure 7 Comparison of phase diagrams of PVA/B(OH)₃/NaOH system: —, observed; ---, calculated

value results, due to domination of the repulsive interaction between monocomplexes, i.e., the contribution of the third term of the RHS of equation (9'). The demixing line thus estimated is shown in Figure 7. The calculated demixing lines reproduce the clear–opaque–clear transition, although some deviations from the observed line are seen at low values of b and C . The discrepancy at low b and C values may be explained as follows. At low polymer concentrations ($C \ll C^*$), each PVA chain is localized, since the envelopes of the PVA chains can not fill the whole space of the system. Therefore, the free energy expression based on a mean field assumption as given by equation (9) can not apply to such a low concentration. In reality, the local polymer concentration, C_{local} , is given by

$$\begin{aligned} C_{\text{local}} &\simeq C^* \quad (\text{in a blob containing a polymer}) \\ C_{\text{local}} &= 0 \quad (\text{otherwise}) \end{aligned} \quad (15)$$

According to this localization of the polymer concentration due to the type of connectivity, the other parameters must be re-estimated and the concentration dependence of equation (9) should be modified. The effect of concentration dependence of the crosslinking formation, which reaches C^*C instead of C^2 at the dilute limit, is not taken into account. This may be the reason why the observed and calculated curves disagree at low concentrations. Since the concentration localization effect appears gradually by lowering the polymer concentration in a real system, we have not discussed this effect in detail. As a result, the clear–opaque line merges into the opaque–clear line at low concentrations. This is observed experimentally but can not be predicted theoretically. Based on the simulation of the demixing transition as discussed above, however, we would conclude that the clear–opaque–clear transition is governed by ionic circumstances as well as C and b .

The essential difference between the results of Pezron *et al.*²⁰ (the clear–opaque transition) and those presented in this paper (the clear–opaque–clear transition) is the difference in the ionic strength. The ionic strength of this work is of the order of 0.1 mol l^{-1} , which is much lower

than used in ref. 20 (i.e. 1 mol l^{-1}). The weaker ionic circumstances bring a clear region at high b as a result of the strong repulsive interaction between monodiol complexes.

Added salt effects

The phase diagram shown in Figure 2 may be changed by adding 1 mol l^{-1} of NaCl, which is shown in Figure 8. The opaque region dominates most of the diagram. Figure 9 shows the same phase diagram as Figure 8, with the ordinate expanded 10-fold. This change is explained as follows: the repulsion effect due to monocomplexes is screened by the added salt, resulting in a contraction of PVA chains. In equation (9') and Figure 6, a large amount of added salt reduces v' and the resulting v_{eff}/v

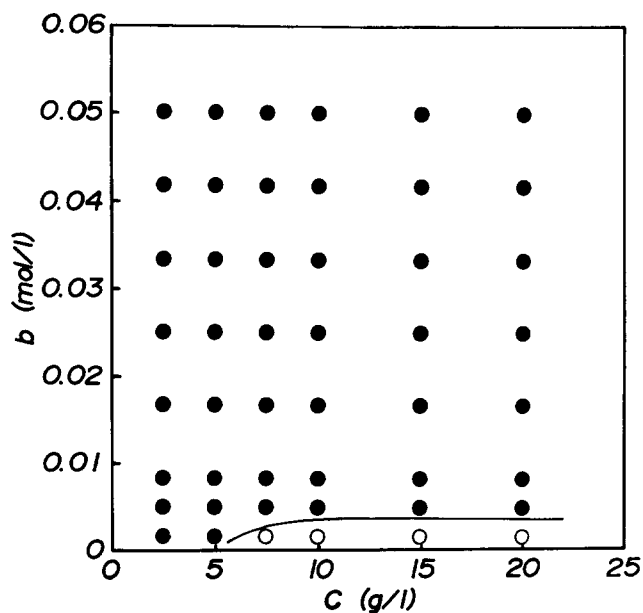


Figure 8 Change in phase diagram of PVA ($P = 1100$)/B(OH)₃/NaOH system by addition of 1 mol l^{-1} NaCl. Comparison should be made with the demixing line in Figure 2 (150 h)

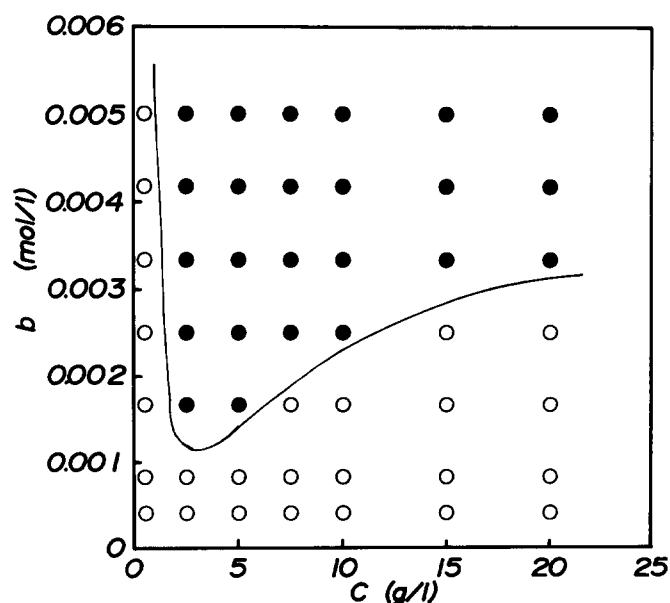


Figure 9 Change in phase diagram of PVA ($P = 1100$)/B(OH)₃/NaOH system by addition of 1 mol l^{-1} NaCl. (Ordinate is ten times that in Figure 8)

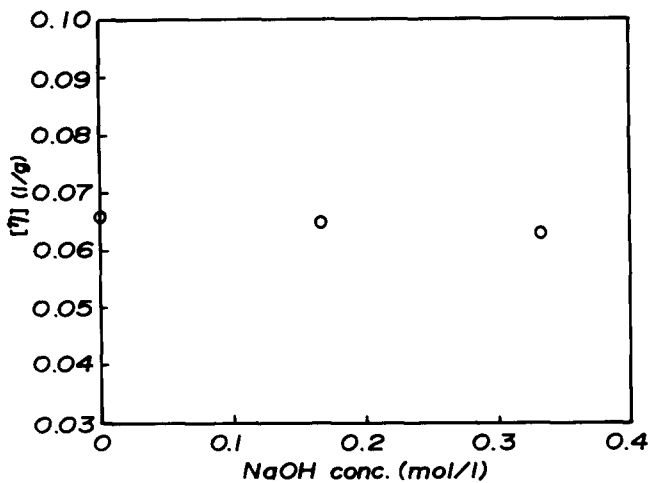


Figure 10 Change in intrinsic viscosity, $[\eta]$, with NaOH concentration. $P = 1800$

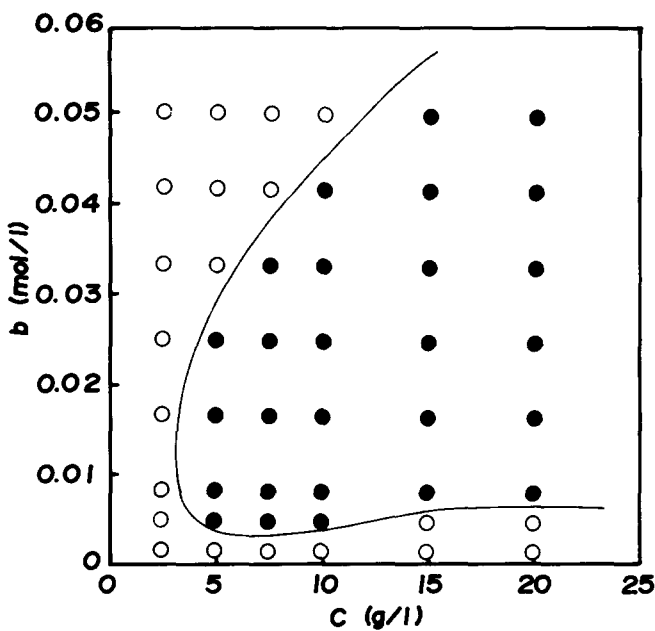


Figure 11 Phase diagram of PVA ($P = 1100$)/ $B(OH)_3$ /NaOH system. NaOH concentration = 0.333 mol l^{-1} . Comparison should be made with the demixing line in Figure 2 (150 h)

remains negative even at high values of b because the recovery from a negative to a positive value of v_{eff}/v is due to the contribution of the term v' .

Figure 9 is very similar to Figure 2 of ref. 17, and shows a clear–opaque transition instead of a clear–opaque–clear transition. It is worth noting that the phase behaviours of each system are very similar, although the polymers are different.

Finally we examine the role of NaOH in this PVA/boric acid/NaOH system. Originally, NaOH was added to control pH so as to obtain an adequate concentration of borate ion. As was discussed earlier, NaOH should also be regarded as an added salt which screens the electrostatic interactions between mono-complex charges. Figure 10 shows the NaOH dependence of the intrinsic viscosity of PVA aqueous solutions. The intrinsic viscosity does not change with NaOH concentration. This result indicates that NaOH does not have any thermodynamic effects on the PVA aqueous solution.

Figure 11 shows the phase diagram of PVA aqueous solutions containing NaOH and $B(OH)_3$ at 17°C . Each solution contains 0.333 mol l^{-1} of NaOH, which is double the value used in Figure 2. A wider opaque region can be found by comparing Figure 11 with Figure 2, particularly at high concentrations of b . This fact supports our supposition that NaOH plays a role as an added salt as well as a reagent for adjusting pH.

Instead of a mixture of NaOH and $B(OH)_3$, borax ($\text{Na}_2\text{B}_4\text{O}_7 \cdot 10\text{H}_2\text{O}$) also produces borate ions. Historically PVA/borax systems have been studied rather than PVA/boric acid/NaOH systems^{4,17–19}. However, the ionic strength of the PVA/borax system is not strong enough to screen out the electrostatic potential between mono-complex charges. No opaque region was observed in the scale of this phase diagram, unless any kind of salt was added to the system.

CONCLUSION

The phase behaviour of PVA aqueous solutions in the presence of boric acid and sodium hydroxide varies with the concentrations of boric acid, PVA, NaOH, and added salt. A clear–opaque–clear transition was observed by increasing boric acid concentration. At PVA concentrations close to the chain overlap concentration, C^* , a sol–gel transition was also observed. The sol–gel transition was found to be very close to C^* by comparing the results of sol–gel transition and intrinsic viscosity measurements. The individual PVA chain dimension and the phase behaviour are governed by complexation of PVA chains and borate ions. At low boric acid concentrations, intra-chain crosslinking formation is dominant, resulting in chain contraction. By further increase in b , monodiol complexation becomes dominant, which leads to chain expansion due to repulsive interactions between the monodiol complexes in a chain. The electrostatic repulsion was removed by adding salt to the system.

A direct evaluation of the individual chain dimension at the demixing zone by means of small angle neutron scattering is now in progress.

ACKNOWLEDGEMENTS

This work was supported in part by a grant-in-aid, Monbsho International Research Program, Joint Research (No. 63044083).

REFERENCES

- 1 Matsuzawa, S., Yamaura, K., Maeda, R. and Ogasawara, K. *Makromol. Chem.* 1979, **180**, 229
- 2 Matsuzawa, S., Yamaura, K. and Kobayashi, H. *Colloid & Polym. Sci.* 1981, **259**, 1147
- 3 Komatsu, M., Inoue, T. and Miyasaka, K. *J. Polym. Sci., Polym. Phys. Ed.* 1986, **24**, 303
- 4 Sinton, S. *Macromolecules* 1987, **20**, 2430
- 5 Yamaura, K., Takahashi, T., Tanigami, T. and Matsuzawa, S. *J. Appl. Polym. Sci.* 1987, **33**, 1983
- 6 Shibayama, M., Sato, M., Kimura, Y., Fujiwara, H. and Nomura, S. *Polymer* 1988, **29**, 336
- 7 Shibayama, M., Yoshizawa, H., Kurokawa, H., Fujiwara, H. and Nomura, S. *Polymer* 1988, **29**, 2066
- 8 Kaji, K., Urakawa, H., Kanaya, T. and Kitamaru, R. *J. Phys. (Paris)* 1988, **49**, 993
- 9 Fujiwara, H., Shibayama, M., Chen, J. and Nomura, S. *J. Appl. Polym. Sci.* 1989, **37**, 1403

- 10 Kaji, K., Kanaya, T. and Ohkura, M. *Polym. Prep. Jpn.* 1989, **38**, 3811
- 11 Wu, W., Shibayama, M., Roy, S., Kurokawa, H., Coyne, L. D., Nomura, S. and Stein, R. S. *Macromolecules* 1990, **23**, 2246
- 12 Deuel, H. and Neukom, A. *Makromol. Chem.* 1949, **3**, 113
- 13 Crisp, J. D. *US Patent 258193*, 1946
- 14 Saito, S. and Okuyama, H. *Kolloid Z.* 1954, **139**, 150
- 15 Ahad, E. J. *Appl. Polym. Sci.* 1974, **18**, 1587
- 16 Pezron, E., Leibler, L., Ricard, A., Lafuma, F. and Audebert, R. *Macromolecules* 1989, **22**, 1169
- 17 Pezron, E., Ricard, A., Lafuma, F. and Audebert, R. *Macromolecules* 1988, **21**, 1126
- 18 Leibler, L., Pezron, E. and Pincus, P. A. *Polymer* 1988, **29**, 1105
- 19 Ochiai, H., Kurita, Y. and Murakami, I. *Makromol. Chem.* 1984, **185**, 167
- 20 Pezron, E., Leibler, L., Ricard, A., Lafuma, F. and Audebert, R. *Macromolecules* 1988, **21**, 1121
- 21 Shibayama, M., Kurokawa, H., Nomura, S., Muthukumar, M., Stein, R. S. and Wu, W. *Polym. Prepr. Jpn.* 1990, **39**, 1276
- 22 Shibayama, M., Muthukumar, M., Kurokawa, H., Roy, S., Nomura, S. and Stein, R. S. *Polymer* submitted for publication
- 23 Coniglio, A., Stanley, H. E. and Klein, W. *Phys. Rev. Lett.* 1979, **42**, 518
- 24 Stauffer, D., Coniglio, A. and Adam, M. *Adv. Polym. Sci.* 1982, **44**, 103
- 25 Pezron, E., Leibler, L. and Lafuma, F. *Macromolecules* 1989, **22**, 2656
- 26 Kurokawa, H., Wu, W. and Shibayama, M. unpublished data
- 27 Shibayama, M., Kurokawa, H., Nomura, S., Roy, S., Stein, R. S. and Wu, W. *Macromolecules* 1990, **23**, 1438